Molecular interactions in nanocellulose assembly

Yoshiharu Nishiyama

Molecular interactions at play in nanocellulose assembly

Yoshiharu Nishiyama

CNRS, CERMAV, F-38000 Grenoble, France, orcid.org/0000-0003-4069-2307

Keywords: hydrogen bond, dispersion force, hydrophobic interaction, cellulose, crystal structure,

Summary

The contribution of hydrogen bond and London dispersion force in the cohesion of cellulose is discussed in light of structure, spectroscopic data, empirical molecular modelling parameters and thermodynamics data of analogue molecules. The hydrogen bond of cellulose is mainly electrostatic, and the stabilization energy in cellulose for each hydrogen bond can be estimated between 17- 30 kJ/mol. In average, hydroxyl groups of cellulose form hydrogen bond comparable to other simple alcohols. London dispersion interaction can be estimated from empirical attraction terms in molecular modelling by simple integration over all components. Although this interaction extends to relatively large distances in colloidal system, the short-range interaction is dominant for the cohesion of cellulose, and is equivalent to a compression of 3 GPa. Trends of heat of vaporization of alkyl-alcohols and alkanes suggests a stabilization by such hydroxyl-group hydrogen bonding to be of the order of 24 kJ/mol, while London dispersion force contributes to about 0.41 kJ/mol/dalton. Simple arithmetic gives good agreement with experimental enthalpy of sublimation of small sugars, where the major cohesive energy comes from hydrogen bonds. For cellulose, due to the reduced number of hydroxyl groups, London dispersion force would be the major component in intermolecular cohesion.

Introduction

The use and transformation of cellulose or “nanocellulose” rely on molecular interactions at the bottom level as any other material and processing. The processing consists of loosening or overcoming the cohesive interaction in order to reshape, and re-arrange typically using various solvents or swelling agents. The ultimate mechanical properties at use are then governed by the topological distribution and strength of molecular interactions. Despite numerous studies on the details of structure and interactions of cellulose, the contributions of different types of interactions in overall properties are rarely discussed in quantitative way.

The most often mentioned molecular interaction of cellulose is “hydrogen bonding”, probably as it is experimentally most demonstrative interactions: hydroxyl groups in the crystal structure in general find its counter part to form favorable electrostatic interaction, and the hydroxyl group stretching bands are red shifted compared to the isolated hydroxyl groups. A recently revived notion is the hydrophobicity and amphiphilicity of cellulose [1] in criticism to recent cellulose-related publications overemphasizing the role of hydrogen bonding against dissolution of cellulose. Still, amphiphilicity or hydrophobic character alone does not explain the solvent resistance, as solvent containing OH and CH groups such as methanol or ethanol barely swells cellulose [2]. Clearly a more quantitative and fine description of molecular interactions at play is needed.

The same is true for the explanation of material properties. “Hydrogen bonding” often serves as a magic word explaining any behavior, such as anisotropic thermal expansion or the Young’s modulus. Although several modeling works are in support of this idea [3], comparison of experimental data on cellulose analogues are less conclusive [4]. London dispersion interactions, arising from temporary polarization is universal but often neglected in cellulose field, except for application of theories of colloids through Hamaker constants [5]. Here I intend to give approximate but quantitative idea on the contribution of hydrogen bond and dispersion interaction on the properties of cellulose.

The hydrogen bond strength in cellulose

Coulomb interactions in molecular modeling

*Author for correspondence (yoshi@cermav.cnrs.fr).

Hydroxyl groups form “weak”[6] or “moderate” hydrogen bonds being mostly electrostatic without significant quantum mechanical charge-transfer, with typical bond energy falling within 16-60 kJ/mol [7]. However, there is no direct way to measure hydrogen bond contribution to the cohesion energy of cellulose. In the molecular modeling, the hydrogen bonds energies are included in the short-range electrostatic interaction in most force fields. For hydrogen bonding with donor (D), hydrogen (H) and acceptor (A) atoms, the Coulomb energy can be simply calculated as

$$E = f\left(\frac{Q_H Q_A}{d_{HA}} + \frac{Q_D Q_A}{d_{DA}}\right)$$

where f = 138.935 KJ nm/mol/e^2 , e being the electron charge. For straight hydrogen bonds, we can assume $d_{DA} \approx d_{HA}+0.1$ (nm). For two hydroxyl groups we can similarly calculate the contribution of four atoms with $d_{DH'} \approx d_{HA}+0.2$, where H’ is the hydrogen on the acceptor oxygen.

Table 1 Partial charges of polar groups in cellulose defined in force-fields

	GROMOS-87	GROMOS-56A	CHARMM-C35	GLYCAM-06
O2	-0.548	-0.642	-0.65	-0.718
HO2	0.398	0.41	0.42	0.437
O3	-0.548	-0.642	-0.65	-0.709
HO3	0.398	0.41	0.42	0.432
O5	-0.360	-0.464	-0.40	-0.471
O6	-0.548	-0.642	-0.65	-0.688
HO6	0.398	0.41	0.42	0.424

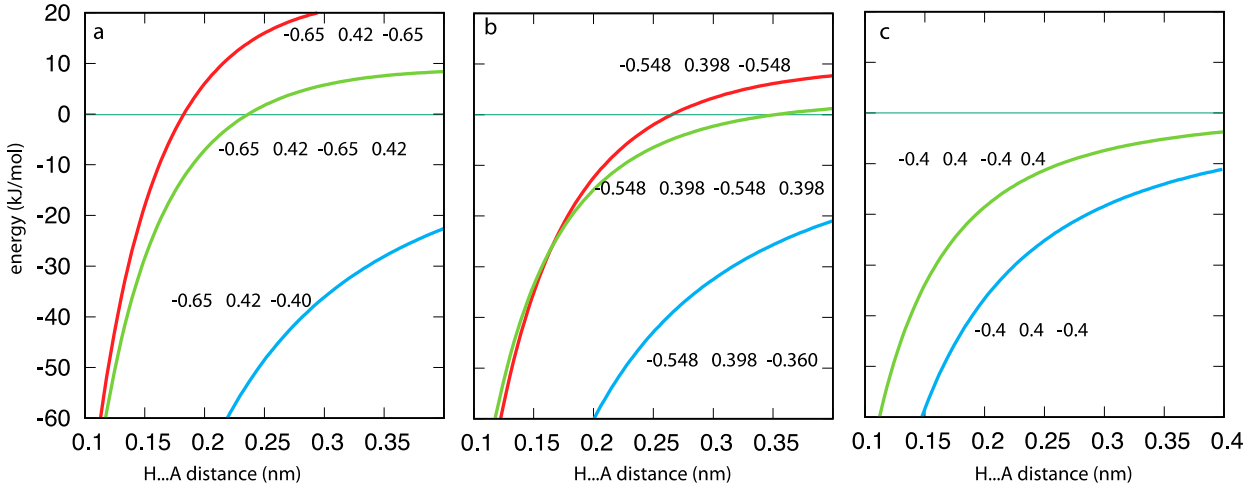

----Figure 1. Electrostatic energy as a function of hydrogen-to-acceptor distance based on partial charges of force field (a) CHARMM-C35, (b) GROMOS-87 and (c)

The partial atomic charges for some popular non-polarizable force fields are listed in table 1. Taking the partial changes of hydroxyl groups, a linear OH…O or OH…OH (taking also the hydrogen attached to acceptor into account) electrostatic energy as function of H…O distance is plotted in red and green respectively in figure 1. Hydroxyl to ring oxygen OH…O is plotted in blue. CHARMM-C35 (a) and GROMOS-87 (b) as well as for a case assuming partial charges of -0.4 0.4 for oxygen and hydrogen (c) were considered. The high energies between the hydroxyl groups at hydrogen bond distances (0.17-0.2 nm) in CHARMM-C35 is due to the net negative charge of the hydroxyl groups, resulting in purely repulsive interaction at longer distance. The older force field, GROMOS-87, rather concentrates charge on the hydroxyl groups resulting in hydrogen bond energy of -18 to -10 kJ/mol for the same distances. On the other hand, the stabilization energy to the ring oxygen is too high in both cases compared to other assessments that will be developed in the following.

Correlation to band shifts of vibrational spectroscopy

An indirect measure of hydrogen bonding energy can be found in the empirical correlation between the heat of formation and infrared band shifts of OH stretching band υ_1[7] or bending band υ_4[8] relative to the isolated molecule (butanol in carbon tetrachloride: υ=3640 and υ_4 = 240 cm^{-1}) . A linear correlation of this $\Delta\nu_1$ to the quantum mechanically calculated interaction energy of amino acid dimers dominated by one hydrogen bond is also reported.[8] In the former, the hydrogen bond energy ΔH is given by

$$\Delta H = 1.3(\Delta \nu_1)^{1/2}$$

$$\Delta H = 0.67 \times 10^{-4} \Delta(\nu ¿¿ 4 ¿¿ 2) ¿¿$$

and in the latter study,

$$\Delta H = 0.0705 \Delta \nu_1$$

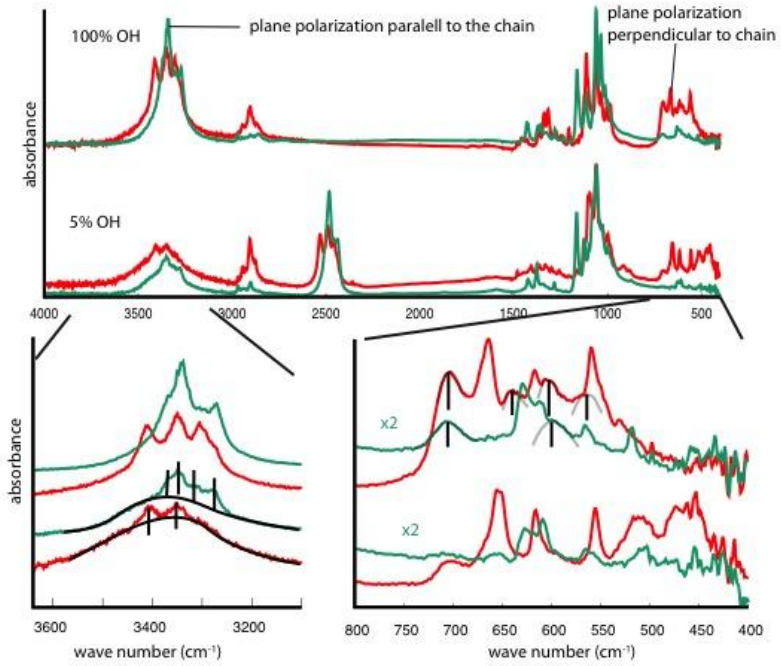

----------Figure 2 Polarized infrared spectra of halocynthia cellulose (a) and its 95 % deuterated sample (b) with plane polarization parallel (green) and perpendicular (red) to the chain.

Figure 2 presents the infrared spectra of uniaxially oriented tunicate cellulose film prepared by the method in ref [9], and isotopically diluted inside the crystals using 95% heavy water according to ref [10]. The infrared spectra from isotopically diluted sample show much simpler bands due to the decoupling of hydrogen bond chains. The tentative assignments are based on the polarization of the bands and the relative H…A distance (Fig. 3) in the structure optimized by using density functional theory with dispersion correction (DFT-D2) using PBE functionals from the neutron crystal structure [11], since the fiber diffraction structure is limited in precision to compare small differences [12]. The hydrogen bond strengths were considered as directly reflecting the hydrogen-to-acceptor distances for assignment.

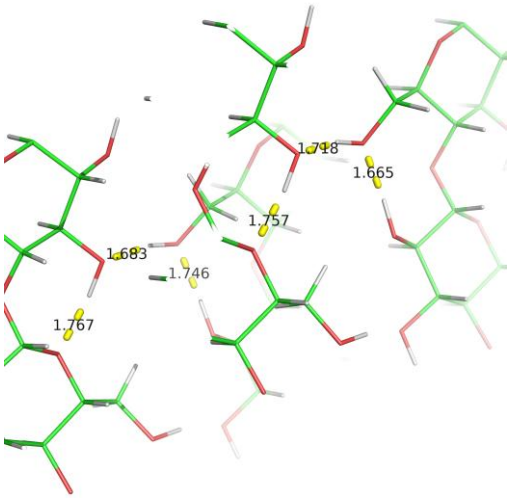

Figure 3 hydrogen bonding distances in DFT optimized cellulose I_β

Table 2 hydrogen bond energies of cellulose I estimated from infrared band shifts

	$H\ldots O_{DFT}$ (Å)	ν1 (cm^{-1})	Δν1 (cm^{-1})	ΔH (kJ/mol)	ΔH (kJ/mol)	ν4 (cm^{-1})	ΔH (kJ/mol)
O3oH…O5o	1.767	3365	275	21.6	19.4	558	17.0
O3cH…O5c	1.757	3350	290	22.1	20.4	603	20.5
O2oH…O6o	1.746	3310	330	23.6	23.3	640	23.6
O2cH…O6c	1.665	3272	368	24.9	25.9	704	29.3
O6oH…O3o	1.683	3350	290	22.1	20.4	704	29.0
O6cH…O3c	1.718	3405	235	19.9	16.6	600	20.6

In any approximation, the hydrogen bond energy values in cellulose I fall between 17 and 30 kJ/mol and intermolecular hydrogen bond would be around 20 kJ/mol. If we consider a 1 -1 0 crystallographic plane the number density of hydrogen bond is roughly $3.7x10^{18}/m^2$, and thus the energy needed to break the hydrogen bonds when splitting the surface would be 20000 x 3.7 $x10^{18}/N_A$ = 0.1 J/m^2. In comparison the fracture energy of wood in mode 1 fracture splitting along the longitudinal direction is of the order of 100 J/m^2 [13], and that of glass is of the order of 5 J/m^2.

Long range dispersion force

The lower bound of long-range dispersion force can be deduced from the experimental evaluation of Hamaker constant on amorphous cellulose of 58 zJ ($z=10^{-21}$)[14]. For two bulk surfaces with 0.12 nm separation (van der Waals radius of hydrogen), the energy will be roughly -0.1 J/m^2, but a reasonable assumption for separation value is not clear.

Table 3. London attraction terms in molecular modeling

		nr[a]	DFT D2	GROMOS43	GROMOS56	Ellipsometry
London attraction coefficient C_6 J nm^6/mol	C	6	1.75	2.34		
	O	5	0.7	2.26	2.26	
	H	10	0.14			
	CH1	5		3.78	6.07	
	CH2	1		7.10	7.47	
	C6H10O5	1	173	277	362	95.7[b]
Hamaker constant (zJ)			104	168	219	58

a: number per residue, b: calculated from Hamaker constant.

In many atomistic molecular modeling, the dispersion force is accounted for by coefficient of London attraction term C_6 in Lennard-Jones potential,

$$E_{LJ}=\frac{C_{12}}{r^{12}}-\frac{C_6}{r^6} \qquad [1]$$

where C_{12} and C_6 are the Lennard-Jones constants and r is the distance between atoms (particles). Recent dispersion corrected density functional theory (DFT) approaches [16] also use this C_6 coefficients which are listed in table 3. Assuming additivity of dispersion interaction, the Hamaker constant A is directly related to the C_6 values [5] and the number density ρ of the atoms (particles) as,

$$A = \pi^2 \rho^2 C_6 \quad [2]$$

For interaction between two different types of atoms i, and j, geometric average $C_{ij} = \sqrt{C_i C_j}$ can be used and thus for system containing multiple types of atoms

$$A = \pi^2 \sum_{i,j} \rho_i \rho_j \sqrt{C_i C_j}. \quad [3]$$

In molecular modeling, the Lennard-Jones interactions are calculated only up to a cutoff-limit, r_c, typically of the order of 1 nm. A long-range dispersion energy E_{lr} above this limit for the bulk can be calculated [17, 18] to compensate the limited cutoff as

$$E_{lr} = \frac{-2\pi}{3} \rho \frac{C_6}{r_c^3} \quad [4]$$

Corresponding to a pressure of

$$P_{lr} = \frac{-4\pi}{3} \rho^2 \frac{C_6}{r_c^3} \quad [5]$$

For example SPC water model with 0.9 nm cutoff gives P_{lr} of about 280 bar (28 MPa).[18]
In the case of nanocellulose, the dimensions are larger than the cutoff, but not necessarily large enough to be considered as bulk. In the following, we should see the effect of crystal size on the London dispersion force.
To simplify the calculation, let us consider each glucosyl residue as the basic element. For glucose residues with long separation compared to its size, inter-atomic distances can be replaced by inter-residue distances, and the dispersion coefficient can be replaced by

$$C_{res} = \sum_{i,j} \sqrt{C_i C_j} \cdot n_i n_j \quad [4]$$

where n_i and n_j are number of atom types in the residue. The values calculated from different dispersion terms varies from 173 – 362 J/mol nm^6 (table 3) while from experimental Hamaker constant of 58 zJ and the number density of residues in cellulose I, 6.08 (1/nm^3) , $C_{res} = 58/\pi^2/6.08^2 = 0.159$ zJ/nm^6 (95.7 J/mol nm^6).
We can approximate cellulose nanocrystal to a cuboid structure where the residues are on a cubic grid with spacing d, making a square cross-section with n_r residues in lateral direction and n_l residues in longitudinal direction, the dispersion energy per residue will be

$$E = \frac{1}{n_r^2 n_l} \frac{1}{2} \sum_i{}' \sum_j{}' \frac{C_{res}}{|di - dj|^6} = \frac{C_{res}}{d^6} \left(\frac{1}{2 n_r^2 n_l} \sum_i{}' \sum_j{}' \frac{1}{|i-j|^6} \right) \quad [5]$$

with the summation over all three dimensional grid points **i, j** (**i**≠**j**). Alternatively, as the dispersion energy between two chains can be approximated by integration as

$$E_c = \frac{3\pi C_{res}}{8 n_r^2 d r^5} + intrachain\,energy \quad [6]$$

where r is the distance between the chains [19]. The summation can be done in two-dimension drastically reducing numerical calculation steps as

$$E' = \frac{C_{res}}{d^6} \left(\frac{3\pi}{8 n_r^2} \frac{1}{2} \sum_p{}' \sum_q{}' \frac{1}{|p-q|^5} + \sum_{i<j}^{n_l} \frac{1}{|i-j|^6} \right) \quad [7]$$

Here, ***p*** and ***q*** are the grid point vectors in the cross-section.

For given chain length and cross-sectional arrangement, the energy is simply proportional to d^{-6} and thus square of the density.

By putting inside the parentheses of eq [5] or [7] as U or U' and d^3 as v (residue volume), the pressure P_{lr}, due to the long-range dispersion forces can be obtained as volume derivative

$$P_{lr} = \frac{dE}{dV} = \frac{C_{res} dU}{dv} \frac{1}{v^2} = \frac{-C_{\Re S}}{2} \frac{U}{v^3} \quad [8]$$

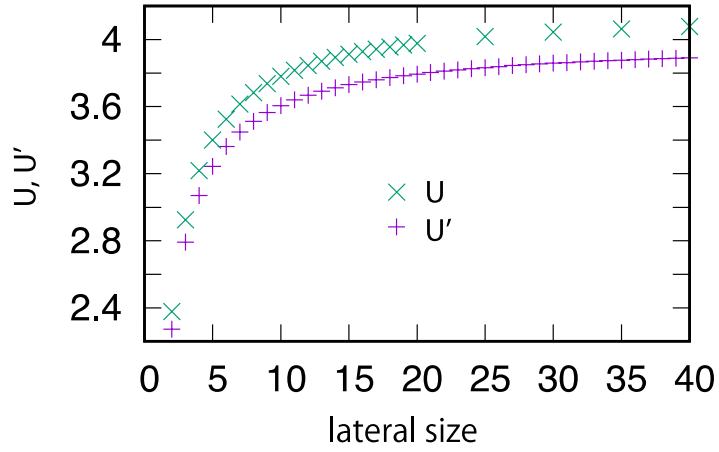

-----figure 4 -------Dimensionless parameter U and U' as a function of lateral sizes

The numerical values of U and U' according to eq 5 and eq 6 using $n_l = 100$ as a function of lateral size in number of residues is plotted in figure 4. The value monotonically increases, and levels off above 20, a typical size of highly crystalline cellulose. For 4x4-chains cross-section, the U value, and hence the energy or pressures is reduced by about 20% compared to the large crystals. For cellulose I, the unit cell containing 4 residues has a volume of 0.658 nm^3, so the volume per residue $v = 0.658/4 = 0.165$ nm^3. The equivalent energy and pressure due to the long-range dispersion attraction is 3.5 kJ/mol(residue) and 69 MPa respectively if we take C_{res} of 95.7 J/mol nm^6.

Effect of dispersion correction on DFT structure

Table 4 The effect of dispersion correction in calculated unit cell parameters

	Volume (Å^3)	a (Å)	b (Å)	c (Å)	γ(°)
exp	658.3	7.784	8.201	10.38	96.6
PBE	744.9	8.70	8.23	10.46	95.5
PBE-D2	642.5	7.65	8.14	10.39	96.8
ε	-0.137	-0.12	-0.011	-0.0067	
σ (GPa)[a]		2.8	4.1	2.9	

a: estimated by using stiffness tensor (c11, c22, c33, c12, c23, c31=21.5, 102.8, 213.3, 13, 11.3,11)[20]

A relatively precise indication of the London dispersion force contribution can be obtained by comparing DFT optimized structure with and without the dispersion correction. In the case of cellulose I_β, the introduction of dispersion term lead to an anisotropic shrinking as listed in table 5 [20]. The stiffness tensor calculated using the same type of functional is reported in the literature [21], and assuming a linear elasticity, the strain due to the dispersion correction can be estimated by multiplying the strain tensor to the stiffness tensor leading to a pressure of 3 - 4 GPa. This pressure is one order of magnitude higher than the effect of the long-range dispersion energy calculated above. Thus the major contribution of dispersion interaction is short-range compared to the residue size. The approximation of using residue center as interaction site largely underestimates the dispersion interaction, due to the highly downward convex nature of $1/r^6$ function at short distances.

Phase change data of analogue molecules

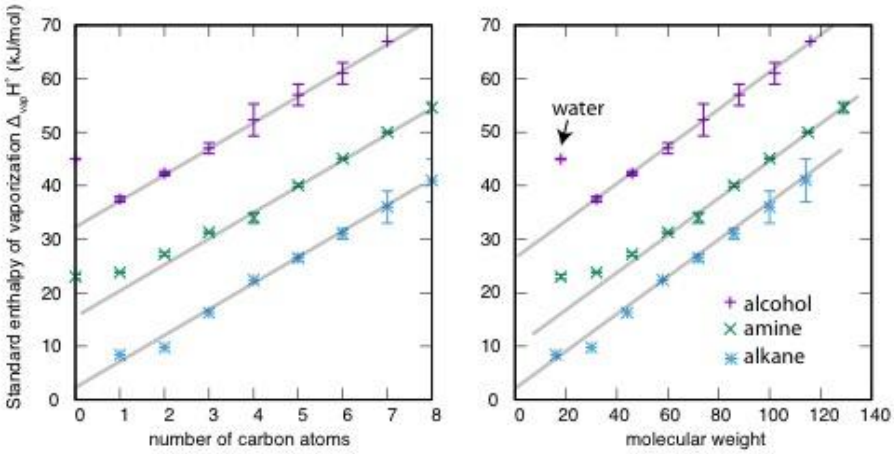

Figure 5 Standard heats of vaporization of linear alkyl alcohols, alkyl amines and alkanes.

An exact calculation of hydrogen bond interaction and dispersion interactions is extremely tedious and prone to error. Instead the hydrogen bond contributions (hydrogen bond increment: δOH) to the heat of evaporation are known to be a good measure of hydrogen bond strength [22, 23]. Figure 5 shows the standard heat of vaporization of linear alkane and normal alcohols and normal alkylamines compiled by National Institute of Standards and Technology of the United States[24]. The heat of vaporization increases linearly with the number of carbon atoms or molecular weights in the same molecular groups but with a shift between alcohols, amines and alkane. If the dispersion interaction from the OH groups were zero, the δOH would be 30 kJ/mol, which is the upper bound. The value will be of the order of 24 kJ/mol from figure 5b assuming that the dispersion energy is simply proportional to molecular weight. The slope in this case is 0.41 kJ/mol/dalton.

Table 5. Heat of vaporization and characteristics of small sugar molecules

	Density (g/cc)	Mw g/mol	n (OH)	$E_{(H\text{-}bond)}$ kJ/mol	E_{disp} kJ/mol	$\%_{(H\text{-}bond)}$	ΔH [25]	ΔH cal
Levoglucosan	1.608	162	3	72	66	52	125 (1)	138
D-xylose	1.524	150	4	96	62	61	158 (3)	158
D-glucose	1.546	180	5	120	74	62	194 (5)	194
Cellobiose	1.56	342	9	216	123	64	301 (44)	339
			8	*192*		*61*		*315*
Cellulose	1.63	162 b	3	72	66	52		138
			2	*48*		*42*		*114*
			1	*24*		*27*		*90*

Based on this empirical relation, we can revisit data on carbohydrates. The heat of sublimation has been reported [25] for a few small sugars as listed in table 5. The experimental heat of vaporization of D-xylose and D-glucose completely agrees with simple addition of dispersion contribution proportional to molecular weight and hydrogen bond contribution proportional to the number of hydroxyl groups in a molecule. Cellobiose and levoglucosan shows slightly lower heat of vaporization compared to this simple arithmetic. Cellobiose forms internal hydrogen bond O3 H…O5 that would remain intact when transferred from condensed phase to vapor phase. Levoglucosan does not forms straight intermolecular hydrogen bond in the crystal [26], but would form O3H…O1 hydrogen bonds in vapor phase [27], and can result in reduced heat of vaporization. These intra-molecular hydrogen bonds, probably strained in the case of levoglucosan, can explain the gap between the experimental value and simple arithmetic.

Extending this empiric relation to cellulose would give an estimate of energy necessary to disperse cellulose in vacuum. In the case of cellulose I, there is only one inter-molecular hydrogen bond per residue, so the energy to isolate one chain would be 90 kJ/mol(residue), or 0.56 kJ/g, compared to 2.4 kJ/g of water. The addition of heat of solvation to this energy would give heat of dissolution. Even taking the two inter-molecular hydrogen bonds in cellulose II and III_I, the hydrogen bond is still the minor component in the cohesion. When we look at linear alcohol (Fig. 5), the dispersion energy contributions exceeds hydrogen bonding only with carbon numbers above 4 (buthanol). The importance of London dispersion energy, proportional to the density, also corroborates with the relative stability among different allomorphs of cellulose [28].

Conclusions

Quantitative, though approximate estimation of hydrogen bonding energy and London dispersion attraction indicates a predominant role of the London dispersion interactions in the cohesion of cellulose. Although London dispersion interaction operates at long distance due to the additivity, the energy short-range interaction between neighbouring residues dominate the overall stabilization.

Additional Information

Information on the following should be included wherever relevant.

Acknowledgment
I thank Pan Chen and Jakob Wohlert for providing me the force-field parameters of cellulose.

Competing Interests
I have no competing interests.

References

[1] Lindman B, Karlström G, Stigsson, L. 2010. On the mechanism of dissolution of cellulose. *J. Mol. Liquid* **156**, 76-81. (doi:10.1016/j.molliq.2010.04.016)
[2] El Seoud OA, Fidale LC, Ruiz N, D'almeida MLO, Frollini E. 2008. Cellulose swelling by protic solvents: which properties of biopolymer and solvent matter? *Cellulose* **15**, 371-392. (DOI 10.1007/s10570-007-9189-x)
[3] Eichhorn SJ, Davies GR. 2006. Modelling the crystalline deformation of native and regenerated cellulose. *Cellulose* **13**, 291-307. (DOI 10.1007/s10570-006-9046-3)
[4] Nishino T, Takano K, Nakamae K. 1999. Elastic modulus of the crystalline regions of chitin and chitosan. *J. Polym. Sci. Part B: Polym. Phys* **37**, 1191-1196. (doi 10.1002/(SICI)1099-0488(19990601)37:11<1191::AID-POLB13>3.0.CO;2-H)
[5] Emsley J. 1980. Very strong hydrogen bonding. *Chem. Soc. Rev.* **9**, 91-124. (doi: 10.1039/CS9800900091)
[6] Jeffrey GA. 1997. An introduction to hydrogen bonding. **Oxford University Press**. (doi)
[7] Bergström L, Stemme S, Dahlfors, T, Arwin H, Ödberg L. 1999. Spectroscopic ellipsometry characterisation and estimation of Hamaker constant of cellulose. *Cellulose* **6**, 1-13. (doi: 10.1023/A:1009250111253)

[8] Wendler K, Thar J, Zahn S, Kirchner B. 2010. Estimating the hydrogen bond energy. *J. Phys. Chem. A* **114**, 9529-9536. (doi: 10.1021/jp103470e)
[9] Nishiyama Y, Kuga S, Wada M, Okano T. 1997 Cellulose microcrystal film of high uniaxial orientation. *Macromolecules* **30**, 6395-6397. (doi: 10.1021/ma970503y).
[10] Nishiyama Y, Isogai A, Okano T, Müller M, Chanzy H. 1999 Intracrystalline deuteration of native cellulose. *Macromolecules* **32**, 2078-2081. (doi: 10.1021/ma981563m)
[11] Nishiyama Y, Langan P, Chanzy H. 2002. Crystal structure and hydrogen-bonding system in cellulose Iβ from synchrotron X-ray and neutron fiber diffraction. *J. Am. Chem. Soc.* **124**, 9074-9082. (doi: 10.1021/ja0257319)
[12] Chen P, Ogawa Y, Nishiyama Y, Bergenstråhle-Wohlert M, Mazeau K. 2015 Alternative hydrogen bond models of cellulose II and III_I based on molecular force-fields and density functional. *Cellulose* **22**, 1485-1493. (doi: 10.1007/s10570-015-0589-z)
[13] Yoshihara H, Kawamura T. 2006. Mode I fracture toughness estimation of wood by DCB test. *Composites A* **37**, 2105-2113.
[14] Bergström L, Stemme S, Dahlfors T, Arwin H, Ödberg L. 1999. Spectroscopic ellipsometry characterisation and estimation of the Hamaker constant of cellulose. *Cellulose* **6**, 1-13.
[15] Hamaker HC. 1937. The London van der Waals attraction between spherical particles. *Physica* **4**, 1058-1071.
[16] Grimme S. 2006. Semiempirical GGA-type density functional construction with a long-range dispersion correction. *J. Comput. Chem.* **27**, 1787-1799.(doi: 10.1002/jcc.20495)
[17] Allen MP, Tildesley DJ. 1987. Computer simulation of liquids. Oxford University Press.
[18] Abraham MJ, van der Spoel D, Lindahl E, Hess B and the GROMACS development team. 2014. GROMACS User Manual version 5.0.4, www.gromacs.org
[19] Salem L. 1962. Attractive forces between long saturated chains at short distances. *J. Chem. Phys* **17**, 2100-2113. (doi: 10.1063/1.1733431)

[20] Bučko T, Hafner J, Lebèque S, Ángyán JG. 2010. Improved Description of the structure of molecular and layerd crystals: Ab Initio DFT calculations with van der Waals corrections. *J. Phys. Chem. A* **114**, 11814-11824. (doi: 10.1021/jp106469x)
[21] Dri FL, Hector Jr. LG, Moon RJ, Zavattieri PD 2013. Anisotropy of the elastic properties of crystalline cellulose I_β from first principles density functional theory with Van der Waals interactios. *Cellulose* **20**, 2703-2718. (doi: 10.1007/s10570-013-00718)
[22] Bondi A, Simkin DJ, 1956 On the Hydrogen Bond Contribution to the Heat of Vaporization of Aliphatic Alcohols, *J. Chem. Phys.* **25**, 1073-1074. (doi: 10.1063/1.1743102)
[23] Bondi A, Simkin DJ, 1957 Heats of vaporization of hydrogen-bonded substances, *AIChE J.* **3**, 473-479. (doi: 10.1002/aic.690030410).
[24] Linstrom PJ and Mallard WG, Eds., NIST Chemistry WebBook, NIST Standard Reference Database Number 69, National Institute of Standards and Technology, Gaithersburg MD, 20899, doi:10.18434/T4D303, (retrieved April 23, 2017).
[25] Oja V, Suuberg EM, 1999 Vapor pressures and enthalpies of sublimation of D-glucose, D-xylose, cellobiose and levoglucosan. *J. Chem. Eng. Data* **44**, 26-29. (doi: 10.1021/je980119b)
[26] Smrčok L, Sládkovičová M, Langer V, Wilson CC, Kóóš M. 2006. On hydrogen bonding in 1, 6-anhydro-β-D-glucopyranose (levoglucosan): X-ray and neutron diffraction and DFT study. *Acta Cryst. B* **62**, 912-918. (doi:10.1107/S010876810602489X)
[27] Rocha IM, Galvão, Sapei E, Ribeiro da Silva MDMC, Ribeiro da Silva MAV. 2013. Levoglucosan : A calorimetric, thermodynamic, spectroscopic, and computational investigation. *J. Chem. Eng. Data* **58**, 1813-1821. (doi : 10.1021/je400207t)
[28] Nishiyama Y, Langan P, Wada M, Forsyth T. 2010. Looking at hydrogen bonds in cellulose. *Acta Cryst. D.* **66**, 1172-1177. (doi:10.1107/S0907444910032397)